

# A multi-purpose reconstruction method based on machine learning for atmospheric neutrinos at JUNO

Hongyue Duyang<sup>1,\*</sup>, Teng Li<sup>1</sup>, Jiayi Liu<sup>2</sup>, Zhen Liu<sup>2</sup>, Wuming Luo<sup>2</sup>, Wing Yan Ma<sup>1</sup>, Xiaohan Tan<sup>1</sup>, Zekun Yang<sup>1</sup>, and Fanrui Zeng<sup>1</sup> on behalf of the JUNO collaboration

<sup>1</sup>Shandong University, Qingdao 266237, People's Republic of China

<sup>2</sup>Institute of High Energy Physics, Beijing 100049, People's Republic of China

**Abstract.** The Jiangmen Underground Neutrino Observatory (JUNO) experiment is designed to measure the neutrino mass ordering (NMO) using a 20-kton liquid scintillator (LS) detector. Besides the precise measurement of the reactor neutrino's oscillation spectrum, an atmospheric neutrino oscillation measurement in JUNO offers independent sensitivity for NMO, which can potentially increase JUNO's total sensitivity in a joint analysis. In this contribution, we present a novel multi-purpose reconstruction method for atmospheric neutrinos in JUNO at few-GeV based on a machine learning technique. This method extracts features related to event topology from PMT waveforms and uses them as inputs to machine learning models. A preliminary study based on the JUNO simulation shows good performances for event directionality reconstruction and neutrino flavor identification. This method also has a great application potential for similar LS detectors.

## 1 Introduction

The Jiangmen Underground Neutrino Observatory (JUNO) [1][2] is currently under construction in southern China. The main physics goal of JUNO is to determine the neutrino mass ordering (NMO). JUNO's central detector (CD, Figure 1) is a 20-kton large-volume liquid scintillator (LS) detector designed to precisely measure the reactor neutrino spectrum from the Taishan and Yangjiang nuclear power plants. The scintillation light produced by neutrino interactions in the JUNO CD is collected by 17612 20-inch photo-multiplier tubes (PMTs) and 25600 3-inch PMTs, providing a total PMT coverage of 78%.

While the JUNO NMO sensitivity is mainly from reactor neutrino oscillations in vacuum, atmospheric neutrino oscillations offer extra sensitivity to NMO via matter effects. A joint analysis of reactor and atmospheric neutrino oscillations can potentially maximize JUNO's total sensitivity. Atmospheric neutrinos are produced by energetic cosmic rays interacting with the upper atmosphere. The atmospheric neutrino flux consists of  $\nu_\mu$ ,  $\bar{\nu}_\mu$ ,  $\nu_e$ , and  $\bar{\nu}_e$ , which can undergo charged current (CC) or neutral current (NC) interactions in the detector. The identification of neutrino flavor is critical for the measurement of oscillation probabilities and the extraction of the oscillation parameters. Besides, the directionality information is also mandatory since it determines the neutrino's oscillation baseline length.

---

\*e-mail: duyang@sdu.edu.cn

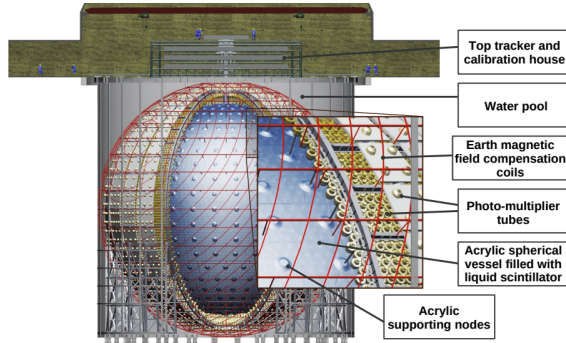


**Figure 1.** Drawing of the JUNO CD design. The homogeneous LS detector is submerged in a water pool that serves as a Cherenkov detector to veto external backgrounds. On the top of the WP is the Top Tracker (TT) detector with plastic scintillators to further help in tagging cosmic ray muons.

However, LS detectors, while offering excellent energy resolution and low threshold and playing an important role in low-energy neutrino physics topics, are traditionally believed to have very limited capability for atmospheric neutrino measurements. This is because those homogeneous detectors do not provide direct tracking information and the Cherenkov light is too weak compared to the scintillation light to give directionality or particle identification information. No measurement of atmospheric neutrino oscillations in an LS detector has ever been reported before.

In this proceeding, we describe a novel method for reconstructing atmospheric neutrinos in an LS detector based on machine learning (ML) techniques. This method starts with extracting features relevant to the event topology in the detector from the PMT waveforms. ML models are trained to learn from these features and output the original event information. We demonstrate that this method can be used for multiple purposes, including the reconstruction of atmospheric neutrinos' directionality, and the identification of their flavors. The performances with Monte Carlo (MC) simulations are presented.

## 2 Methodology

The energy range of atmospheric neutrinos that is most sensitive to NMO is about 1-10 GeV. In this energy region, neutrinos can interact with LS and produce charged particles with enough energy to make tracks with lengths of several tens of centimeters or longer. The space and time distribution of scintillation light photons produced by these charged particles are not isotropic but depend on the detailed event topology in the detector. Figure 2 shows the number of photoelectrons (PEs) as functions of time for PMTs at different angles with respect to a simulated muon track. PMTs at different angles see distinct PE time distributions and therefore have distinct waveforms. The exact shape of the waveform depends on the relative position of the PMT to the particle track as well as the energy deposition ( $dE/dx$ ) along the track. In this study, features are extracted from PMT waveforms in the first 1.25  $\mu s$  readout window to mathematically describe the characteristics of the waveforms that are relevant to the event information. Such features include the time of the earliest photon seen by a PMT (first hit time, FHT), the total charge, the slope of the waveform in the first 4 ns after FHT, the ratio of the charge in the first 4 ns after FHT to the total, the charge and time

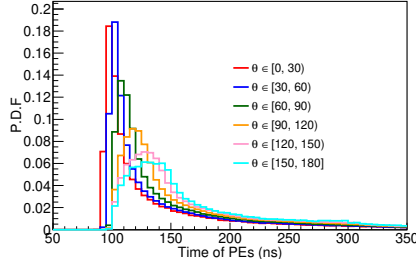


**Figure 2.** Comparison of the normalized PE time distributions between PMTs at different angles with respect to a simulated 1 GeV muon track. Distinct shapes are observed.

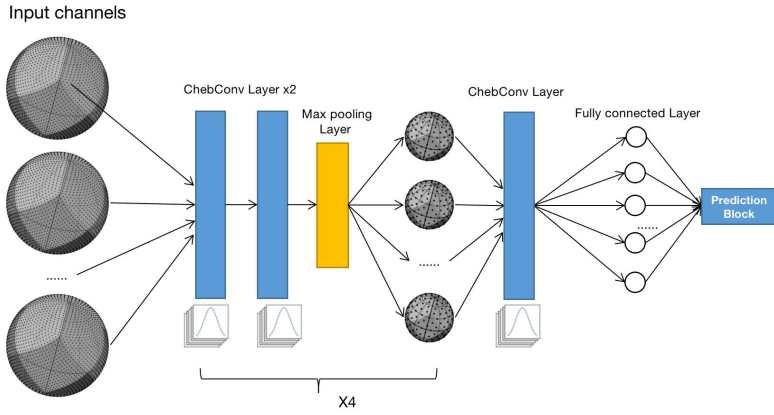


**Figure 3.** The DeepSphere-based model architecture used in this study. The model consists of four blocks, each with two Chebyshev convolution (ChebConv) layer and a max pooling layer, followed by an additional ChebConv layer, a fully connection layer and a prediction block.

of the waveform peak, and others. Those features are used as inputs to ML models. Only features from 20-inch PMTs are used in this study.

Features from all the 20-inch PMTs on the inner surface of the JUNO CD form spherical images-like data. Three different types of ML models are developed to process such data. The first is a planar model based on EfficientNetV2 [3]. It inputs pictures formed by projecting features of each PMT onto a 2D  $\theta_{PMT}$  and  $\phi_{PMT}$  grid, where  $\theta_{PMT}/\phi_{PMT}$  is the zenith/azimuth angles of the PMT position. The second is a spherical model, based on DeepSphere [4], which deals with spherical images. The third is a 3D model based on PointNet++ [5] which inputs the PMT features as 3D point clouds. The structure of the DeepSphere-based model is shown in Figure 3. The structures of the EfficientNetV2-based and PointNet++-based models are taken from [3] and [5] with minor modifications.

The dataset used in this study is simulated with the official JUNO software with complete detector and electronic effects. The GENIE neutrino event generator [6][7] is used to simulate  $\nu_{\mu}/\bar{\nu}_{\mu}$ -CC,  $\nu_e/\bar{\nu}_e$ -CC and NC interactions with neutrino flux from [8].

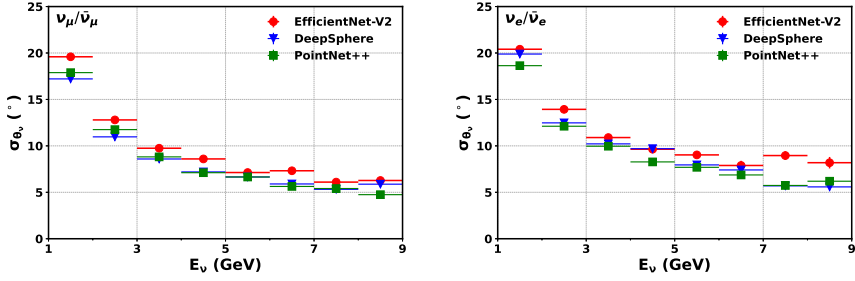


**Figure 4.** The  $\theta_v$  resolutions are shown as functions of neutrino energy  $E_\nu$  for  $\nu_\mu/\bar{\nu}_\mu$ -CC (left) and  $\nu_e/\bar{\nu}_e$ -CC events (right) using the three ML models.

### 3 Performances

Both the neutrino directionality reconstruction and flavor identification performances are reported in this proceeding. The models described in section 2 are trained by the simulated dataset separately for these two purposes. 80% of the dataset is used for model training with the rest 20% for validation. The results of the validation sample are quoted as the performances of reconstruction and event identification.

#### 3.1 Directionality

In the case of directionality reconstruction, a directional unit vector representing the incoming neutrino direction is chosen as the model output. The loss function is the Euclidean distance between the true and reconstructed endpoint of the vector. The angular resolution is defined as one standard deviation of the Gaussian fitted difference between the true and reconstructed zenith angles of the neutrino ( $\theta_v$ ) in 1 GeV neutrino energy bins. Figure 4 shows the resolutions as functions of neutrino energy for all three models, with  $\nu_\mu/\bar{\nu}_\mu$ -CC and  $\nu_e/\bar{\nu}_e$ -CC evaluated separately. Overall the three models show comparable performances, which improve with increasing neutrino energy. It is also noticeable that the performance of  $\nu_\mu/\bar{\nu}_\mu$ -CC is slightly better than  $\nu_e/\bar{\nu}_e$ -CC, which is understandable since the (anti)muons in the final state of  $\nu_\mu/\bar{\nu}_\mu$ -CC interactions generally provide better directional information than the electrons/positrons in the  $\nu_e/\bar{\nu}_e$ -CC case which showers in the LS detector.

#### 3.2 Flavor identification

A 3-label classification is reported for the neutrino flavor identification. The three categories are  $\nu_\mu/\bar{\nu}_\mu$ -CC,  $\nu_e/\bar{\nu}_e$ -CC and NC events. Note that the neutrino versus anti-neutrino identification is also possible with Michel electron and neutron capture information. Michel electrons and captured neutrons produce delayed triggers after the prompt trigger. Only results obtained from the prompt trigger (the first 1250  $\mu$ s) features are reported in this proceeding. The ML models again show comparable performances. The selection efficiency and purity of the two signal samples,  $\nu_\mu/\bar{\nu}_\mu$ -CC and  $\nu_e/\bar{\nu}_e$ -CC, are shown in Figure 5 using the DeepSphere result as an example. Both the efficiency and purity improve as energy increases below 3 GeV, and then get worse when the energy is above 5 GeV. This could be explained by the fact that at low energies the track lengths of (anti)muons or electrons/positrons are too short in the final state

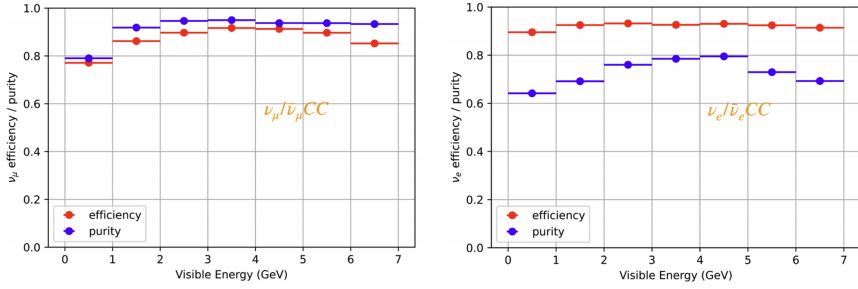


**Figure 5.** Selection efficiency (red) and purity (blue) of the  $\nu_\mu/\bar{\nu}_\mu$ -CC (left) and  $\nu_e/\bar{\nu}_e$ -CC (right) events as functions of event visible energy in this study.

of  $\nu_\mu/\bar{\nu}_\mu$ -CC and  $\nu_e/\bar{\nu}_e$ -CC interactions, while at higher energy, the NC interactions tend to produce energetic charged or neutral pions which mimic (anti-)muons or electrons/positrons in LS and make the identification more difficult.

## 4 Summary

A multi-purpose reconstruction method for atmospheric neutrinos in JUNO is presented. Both the directionality reconstruction and flavor identification show promising results cross-checked by different ML models. This is the first time that these goals have been achieved in a homogeneous LS detector with MC simulation, making a future atmospheric neutrino oscillation measurement in JUNO possible. While developed for JUNO, this method is in principle applicable to other LS detectors and other physics topics in the GeV energy region as well, which can greatly expand the application of LS detectors in particle physics.

## Acknowledgements

This work is supported by the National Natural Science Foundation of China (Grant No.12275160, No.12105158, No.12025502), the Science Foundation of Shandong Province (Grant No. ZR2022MA062) and the China Postdoctoral Science Foundation (Project No. 2202M713153).

## References

- [1] F. An et al. (JUNO Collaboration), *J. Phys. G* **43**, 030401582 (2016).
- [2] A. Abusleme et al. (JUNO Collaboration), *Prog. Part. Nucl. Phys.* **123**, 103927 (2022).
- [3] M. Tan and Q. Le, in *Proceedings of the 38th International Conference on Machine Learning*, Proceedings of Machine Learning Research, Vol. 139 (PMLR, 2021) pp.10096–10106.
- [4] N. Perraudin, M. Defferrard, T. Kacprzak, and R. Sgier, *Astronomy and Computing* **27**, 130 (2019).
- [5] C. R. Qi, L. Yi, H. Su, and L. J. Guibas, in *Advances in Neural Information Processing Systems*, Vol. 30 (Curran Associates, Inc., 2017).
- [6] C. Andreopoulos, C. Barry, S. Dytman, H. Gallagher, T. Golan, R. Hatcher, G. Perdue, and J. Yarba, (2015), arXiv:1510.05494 [hep-ph].

- [7] Tena-Vidal et al. (GENIE Collaboration), Phys. Rev. D **104**, 072009 (2021).
- [8] M. Honda, M. S. Athar, T. Kajita, K. Kasahara, and S. Midorikawa, Phys. Rev. D **92**, 023004 (2015).